



Mesoporous silica materials modified with alumina polycations as catalysts for the synthesis of dimethyl ether from methanol



Daniel Macina^a, Zofia Piwowarska^a, Karolina Tarach^a, Kinga Góra-Marek^a, Janusz Ryczkowski^b, Lucjan Chmielarz^{a,*}

^aJagiellonian University, Faculty of Chemistry, Ingardena 3, 30-060 Kraków, Poland

^bMaria Curie-Skłodowska University, Faculty of Chemistry, Maria Curie-Skłodowska 2, 20-031 Lublin, Poland

ARTICLE INFO

Article history:

Received 18 July 2015

Received in revised form 28 October 2015

Accepted 9 November 2015

Available online 12 November 2015

Keywords:

nanostructures

chemical synthesis

nuclear magnetic resonance (NMR)

transmission electron microscopy (TEM)

catalytic properties

ABSTRACT

Mesoporous silica materials (SBA-15 and MCF) were used as catalytic supports for the deposition of aggregated alumina species using the method consisting of the following steps: (i) anchoring 3-(mercaptopropyl)trimethoxysilane (MPTMS) on the silica surface followed by (ii) oxidation of —SH to —SO₃H groups and then (iii) deposition of aluminum Keggin oligocations by ion-exchange method and (iv) calcination. The obtained samples were tested as catalysts for synthesis of dimethyl ether from methanol. The modified silicas were characterized with respect to the ordering of their porous structure (XRD), textural properties (BET), chemical composition (EDS, CHNS), structure (²⁷Al NMR, FTIR) and location of alumina species (EDX-TEM), surface acidity (NH₃-TPD, Py-FTIR) and thermal stability (TGA). The obtained materials were found to be active and selective catalysts for methanol dehydration to dimethyl ether (DME) in the MTD process (methanol-to-dimethyl ether).

© 2015 Elsevier Ltd. All rights reserved.

1. Introduction

Mesoporous silica materials, which were first synthesized by scientists from Mobil in 1992, have been intensively studied with regards to their technical applications in different areas including catalysis and adsorption [1–3]. Such materials, characterized by a very high specific surface area and pore volumes, ordered porous structure as well as high thermal and hydrothermal stability, can be synthesized by surfactant directed methods using various types of surfactants [3,4]. However, one of the main drawback of the pure mesoporous silicas is the lack of ion-exchange properties, what limits possibility of the uniform deposition of catalytically active components in a simple way.

Thus, in most cases, more advanced procedures are required to activate the surface towards specific catalytic purposes [5]. The activation is typically performed by incorporation of heteroelements into the silica framework or by their deposition on the silica surface. One of the method resulting in uniform dispersion of the catalytically active components on the silica surface is their grafting based on the formation of chemical bounds between elements located on the silica surface and molecules of active species precursors [e.g. 5–8]. These methods are relatively well

developed for deposition of catalytically active components in the form of mononuclear species [e.g. 5–8], while there is a lot of processes in which aggregated metal oxide species are active. Therefore, the studies focused on deposition of aggregated Al₂O₃ species on the high-surface area mesopores silica were undertaken. The obtained materials were tested in the role of catalysts for the synthesis of dimethyl ether (DME) from methanol.

Dimethyl ether (DME), the simplest of the ethers, is one of the most promising environmentally benign and economic alternative fuel for the future applications [9–11]. DME is commonly used as an aerosol propellant in cosmetics industry, coolant, key intermediate for the production of many important chemicals (such as dimethyl sulfate or methyl acetate), source of hydrogen for fuel cells, fuel in gas turbines for power generation [9,11–14]. Furthermore, it has similar properties to propane and butane, the principal constituent of LPG, and therefore it can be used as a LPG substitute in domestic energy supply or for industrial uses [11–17]. Another advantage of DME is that it can be used as an additive for diesel fuel due to its high cetane number (about 55–60), high oxygen content (34.8% by mass) and lack of C—C bond [9–17]. Dimethyl ether can be produced in two main routes. The first one is the direct method, in which DME is produced from syngas in the STD process (syngas-to-dimethyl ether) over bifunctional catalysts, consisting of methanol synthesis component as well as methanol dehydration component [9,10,14–16,18,19]. The second route is based on indirect method, in which

* Corresponding author.

E-mail address: chmielar@chemia.uj.edu.pl (L. Chmielarz).

methanol is firstly synthesized and then, after purification, converted to DME in another reactor over solid acid catalysts in the MTD process (methanol-to-dimethyl ether) [9,14–19]. DME synthesis from alcohol is known as an acid catalyzed and exothermic reaction. Commercial catalysts, typically used for the MTD process, are solid acid materials, such as γ -Al₂O₃, zeolites (HZSM-5 or HY), silica-alumina or phosphorus-alumina [11,12,15–19]. It has been reported in the open literature that the total acidity of the catalyst is a crucial parameter which determines distribution of the obtained products in this process [16,18,20]. Many reaction mechanisms have been suggested by scientists for methanol dehydration [21–23]. However, it is generally accepted that Brønsted as well as Lewis acid sites catalyze this reaction, depending on the applied catalyst [24,25]. The reaction mechanisms suggested in literature can be classified into two main groups: Eley-Rideal (ER) and Langmuire-Hinshelwood (LH). The former mechanism assumes that only acidic sites are active in this process [e.g. 26–28]. According to this mechanism, in the first step acid site located on the surface of catalyst reacts with nucleophilic oxygen of methanol molecule. In the next stage an intermediate surface species reacts with a gas-phase molecule what results in the formation of DME. On the other hand, LH mechanism assumes that both acidic (noted as H⁺) and basic (O²⁻) sites are active during the dehydration process forming from two methanol molecules [CH₃·OH₂]⁺ and [CH₃O]⁻ species on H⁺ and O²⁻, respectively [e.g. 23,26]. Finally, after condensation, one DME molecule and one water molecule are produced.

Another important factor, affecting distribution of the obtained products, is the porosity of the catalyst. It was reported in the literature, that zeolites deactivated quickly, due to strong acidity and coke formation in micropores [9,15,29]. Mesoporous materials, characterized by larger pores than zeolites, are considered to be much less susceptible to deactivation due to much less diffusion limitations in their pore systems [17,30].

The main goal of the presented studies was preparation of effective high surface area catalysts for the DME synthesis from methanol. Therefore as supports mesoporous silica materials (SBA-15, MCF) were used. Acidic properties were generated by controlled deposition of alumina oligocations, which during calcination formed alumina aggregates known to be active in the DME synthesis. Such strategy of the catalyst preparation resulted in high surface area materials characterized by large surface concentration of acid sites of moderate strength, what is important in the process of DME synthesis.

2. Experimental

2.1. Catalysts preparation

Mesoporous silicas (SBA-15 and MCF) were used as supports for deposition of alumina species to generate surface acidity. SBA-15 was synthesized according to the slightly modified procedure described earlier by Chmielarz et al. [6]. 4 g of Pluronic P123 triblock copolymer surfactant (EO20-PO70-EO20, Sigma-Aldrich) was dissolved in 30 g of distilled water and 120 g of 2 M HCl (37%, Sigma-Aldrich). Subsequently, a suitable amount of tetraethyl orthosilicate (TEOS, Sigma-Aldrich) was added. The obtained suspension was stirred at 40 °C for 20 h and then aged at 90 °C for 24 h. The solid product was separated by filtration, washed with distilled water and dried at 60 °C for 8 h. Finally, the obtained sample was calcined in an air atmosphere at 550 °C with a heating rate of 1 °C/min and an isothermal period of 6 h.

The synthesis method of MCF was given previously by Meynen et al. [31]. 4.0 g of Pluronic P123 was dissolved in 150 mL of 1.6 M HCl at 35 °C. Then, 0.0467 g of NH₄F (Sigma-Aldrich) and 4.6 mL of 1,3,5-trimethylbenzene (mesitylene, Sigma-Aldrich) were added

and vigorously stirred at 40 °C for 1 h. Subsequently, 9.14 mL of TEOS was added and the obtained suspension was stirred at 40 °C for 20 h. Then, the slurry was transferred to an autoclave and aged at 100 °C for 24 h. The obtained precipitate was filtered, washed with distilled water and dried at 60 °C for 8 h. Finally, the obtained sample was calcined in an air atmosphere at 550 °C with a heating rate of 1 °C/min and an isothermal period of 6 h.

In the next step the surface of mesoporous silicas was modified with organic species to generate ion-exchange properties. The silica samples were functionalized with organic groups according to the procedure described earlier by Trejda et al. [32] with some modifications. Both SBA-15 and MCF, before modification step, were thermally treated at 200 °C for 2 h in order to remove surface adsorbed water. Then, in each case 2 g of mesoporous silica was dispersed in 50 mL of zeolite (ZSM-5) dried toluene (POCH). The obtained mixtures were heated to 110 °C and intensively stirred for 30 min. Subsequently, 3.7 mL of 3-(mercaptopropyl) trimethoxysilane (MPTMS, Sigma-Aldrich) was added and the obtained mixtures were intensively stirred at 110 °C for next 24 h. After filtration the modified materials were successively washed with toluene (150 mL), ethanol (150 mL, POCH) and distilled water (700 mL). Finally, the samples were dried at 60 °C for 8 h. The obtained samples are denoted as SBA-15-SH and MCF-SH. In the next step SBA-15 and MCF with anchored MPTMS were treated with a solution of H₂O₂ (POCH) in order to oxidase —SH groups to —SO₃H. 2 g of modified silica was dispersed in 30% aqueous solution of H₂O₂ (40 mL). The obtained slurry was stirred at room temperature (RT) for 24 h. In the next step, the sample was separated by filtration, washed with distilled water and ethanol and finally dried at 60 °C for 8 h. The obtained samples are denoted as SBA-15-SO₃H and MCF-SO₃H.

The modified silicas (SBA-15-SO₃H and MCF-SO₃H) were doped with aluminum oligocations (Al¹³, [Al₁₂(AlO₄)(OH)₂₄(H₂O)₁₂]⁷⁺). The solution of aluminum oligocations was prepared according to the procedure applied in our previous studies [33]. An appropriate volume of 0.1 M aqueous solution of NaOH was slowly added into AlCl₃ solution under constant stirring until the molar ratio of OH⁻/Al³⁺ reached the value of 2.4. The obtained solution was aged at RT for two weeks. Then, such aged solution of aluminum oligocations was slowly added into suspension containing 1 wt.% of SBA-15-SO₃H or MCF-SO₃H dispersed in distilled water until the Al³⁺/modified silica ratio reached the value of 10 mmol Al³⁺/g modified silica. The obtained mixture was vigorously mixed at RT for 24 h. In the next step the solid product was separated by filtration, washed with distilled water until complete removal of chloride anions and dried at 120 °C for 12 h. Finally, the samples were calcined at 500 °C for 12 h with a heating rate of 1 °C/min. The obtained samples are denoted as SBA-15-SO₃H-Al and MCF-SO₃H-Al.

2.2. Characterization methods

The X-ray diffraction patterns of the samples were recorded using a Bruker D2 Phaser diffractometer. The measurements were performed in the 2 theta range of 0.4 - 10° with a step of 0.02° using Cu-K α radiation ($\lambda = 1.54056 \text{ \AA}$).

Textural parameters of the samples were determined by N₂ adsorption at -196 °C using a 3Flex (Micromeritics) automated gas adsorption system. Prior to the analysis, the samples were outgassed under vacuum at 350 °C for 24 h. The specific surface area was determined using the BET equation. The total volume of pores (at $p/p_0 = 0.98$) was calculated using the single point model. Mesopore size distributions were determined using the BJH model.

The efficiency of surface functional groups anchoring was studied using FT-IR, thermogravimetry and elemental analysis. FT-IR measurements were performed for the samples with grafted

MPTMS (before and after oxidation with H_2O_2) using a Nicolet 6700 FT-IR spectrometer (Thermo Scientific) equipped with DRIFT (diffuse reflectance infrared Fourier transform) accessory and DTGS detector. The dried samples were grounded with dried potassium bromide powder (4 wt.%). The measurements were carried out in the wavenumber range of $650\text{--}4000\text{ cm}^{-1}$ with a resolution of 2 cm^{-1} .

Thermogravimetric measurements were performed using a TGA/SDTA851^e Mettler Toledo instrument connected with quadrupole mass spectrometer ThermoStar (Balzers). The samples were heated in a flow of synthetic air (80 mL/min) with a heating rate of $10^\circ\text{C}/\text{min}$, in the temperature range of $30\text{--}1000^\circ\text{C}$.

The content of carbon and sulfur in the mesoporous supports modified with surface functional groups was determined using a CHNS Vario MICRO Cube microanalyzer.

The chemical composition of the samples was determined by an electron microprobe analysis performed on a JEOL JXA 733 Superprobe (electron probe microanalysis - EPMA).

The STEM images of the alumina modified samples were obtained with the use of a Tecnai Osiris 200 kV TEM/STEM system equipped with HAADF detector and Super-EDX windowless detector. STEM micrographs were coupled with EDX data for the presentation of the chosen elements distribution.

High-resolution solid-state ^{27}Al NMR spectra were recorded on a Bruker 300 MHz Ultra Shield spectrometer operating at 78.172 MHz for ^{27}Al using magic angle spinning (CP/MAS) method. The spinning rate was set at 8000 Hz. Number of scans for investigated samples was in the range 4096–16384. Moreover acquisition time (AQ) was set to 0.016434 s, and relaxation delay (D1) to 0.5 s. For data acquisition was used pulse program

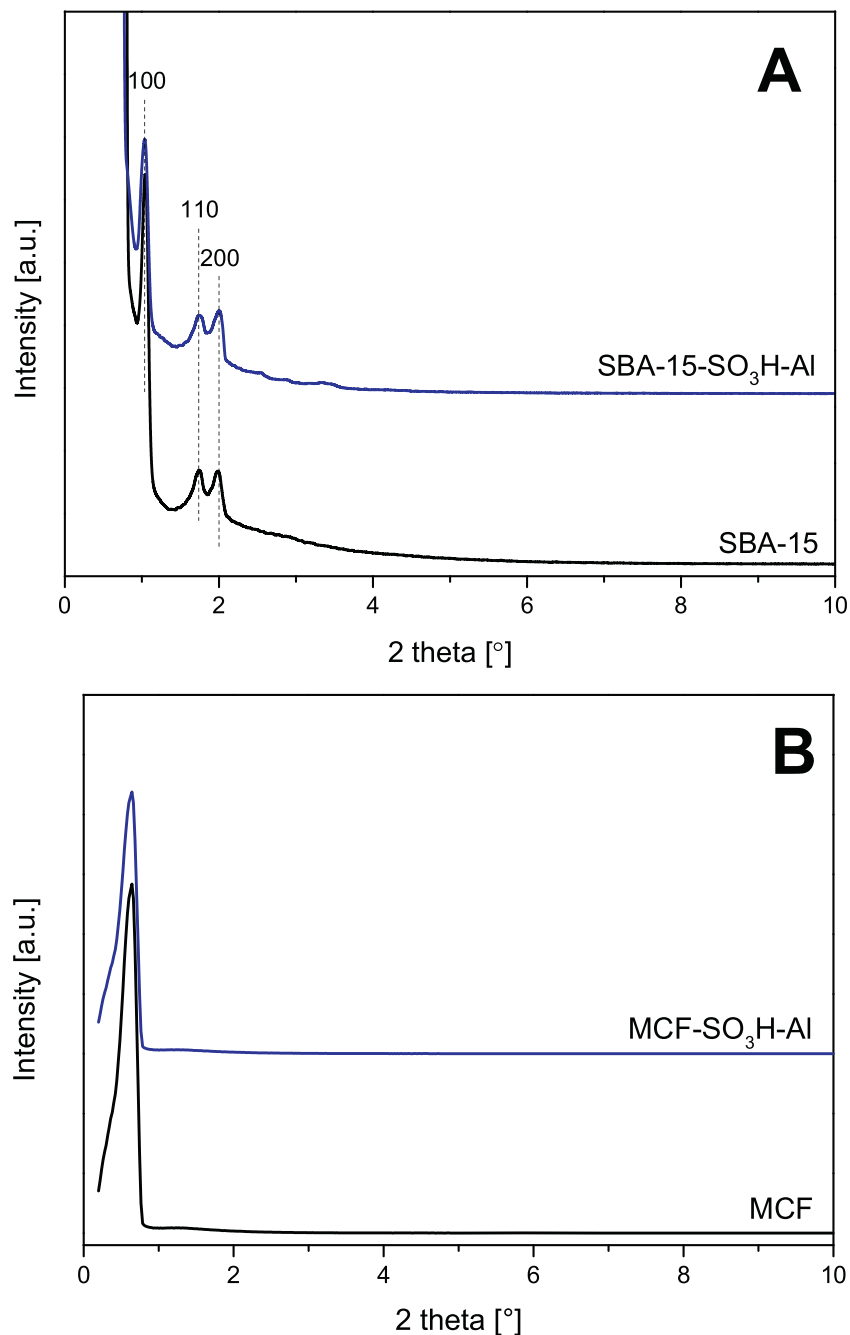


Fig. 1. XRD patterns recorded for the pure silica supports and their modifications with alumina species.

(PULPROG: hpdcc). The measurements were performed at room temperature.

The acidity (concentration and strength of acidic sites) of the samples was studied by temperature-programmed desorption of ammonia (NH_3 -TPD). The measurements were carried out in the temperature range of 70–600 °C in a fixed bed continuous flow microreactor system equipped with QMS detector (PREVAC). Reaction temperature was measured by a K-type thermocouple located in a quartz capillary immersed in the catalyst bed. Before NH_3 -TPD experiments, each sample (50 mg) was outgassed in a flow of pure helium (20 mL/min) at 500 °C for 30 min. Subsequently, the sample was cooled down to 70 °C and saturated in a flow of 1 vol.% of NH_3 diluted in He (20 mL/min) for about 120 min.

Then, the catalyst was purged in a flow of pure helium until a constant baseline level was attained. Desorption was carried out with a linear heating rate (10 °C/min) in a flow of pure helium (20 mL/min). Calibration of quadrupole mass spectrometer with commercial mixtures allowed to recalculate the detector signal into the rate of NH_3 evolution.

Distribution of acid sites of Brønsted and Lewis types and their strength were determined by FTIR analysis of pyridine pre-adsorbed samples. Prior to FTIR studies, the samples were formed into the self-supporting wafers (ca. 5 mg/cm²) and in-situ thermally treated in quartz home-made IR cell at 450 °C under high vacuum for 1 h. Quantitative experiments were carried out with the use of pyridine as a probe molecule. The measurements

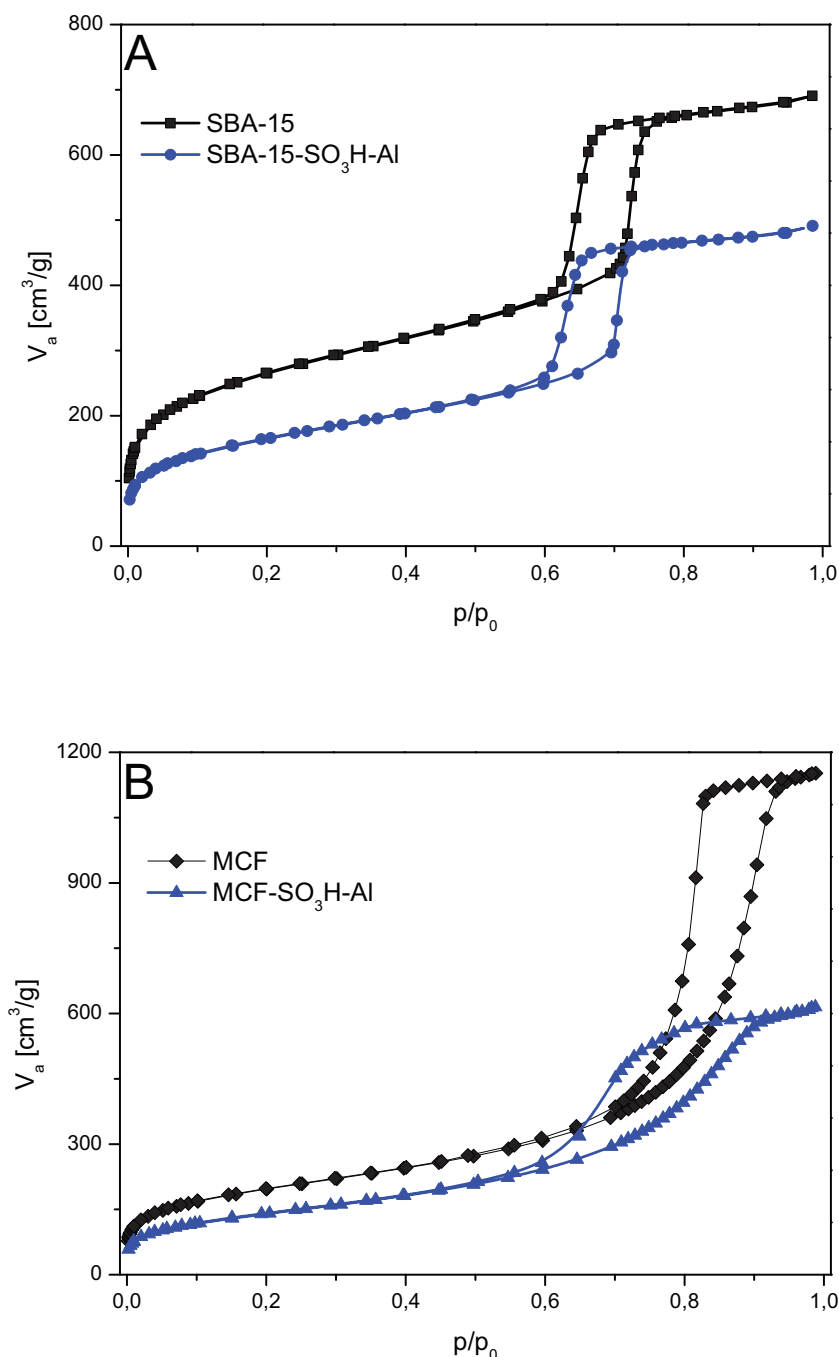


Fig. 2. Nitrogen adsorption-desorption isotherms recorded for the pure silica supports and their modifications with alumina.

Table 1
Textural parameters of mesoporous silica materials and their modifications.

Sample	S_{BET} (m^2/g)	V_p (cm^3/g)	$\langle d \rangle$ (nm)
SBA-15	952	1.070	5.89
SBA-15-SO ₃ H-Al	585	0.761	5.67
MCF	709	1.784	11.85
MCF-SO ₃ H-Al	510	0.953	7.73
γ -Al ₂ O ₃	258		

were realized by saturation of acid sites in the samples with pyridine (POCH) at 130 °C and subsequently, physisorbed pyridine molecules were removed by evacuation at the same temperature for 20 min. The concentrations of both Brønsted and Lewis acid sites were calculated from the maximum intensities of the PyH⁺ and PyL bands and corresponding values of the extinction coefficients [34]. Then, the samples were heated to 330 °C and evacuated for 20 min, before spectrum recording. The relative strength of both Brønsted and Lewis acid sites was determined as the ratio of maximum intensities of the PyH⁺ and PyL bands recorded at 130 °C and 330 °C.

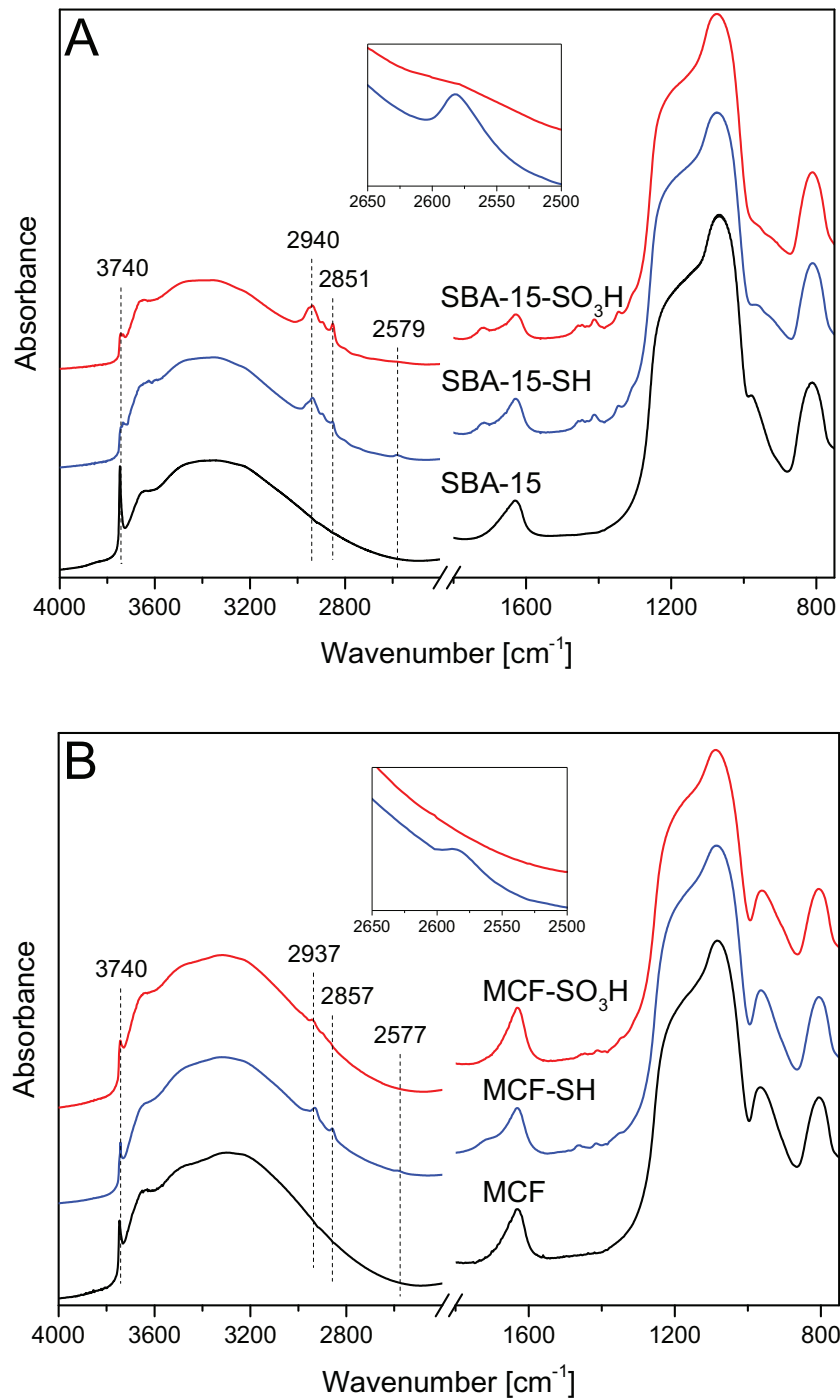


Fig. 3. DRIFT spectra of the pure silica supports and the samples modified with —SH and —SO₃H groups.

2.3. Catalytic studies

Catalytic experiments were performed in a fixed-bed flow quartz microreactor system under atmospheric pressure in the temperature range of 125–300 °C with a step of 25 °C. For each test 100 mg of catalyst with a particle size between 0.160 and 0.315 mm was outgassed in a flow of pure helium at 300 °C for 1 h. After cooling down to 125 °C the gas mixture containing 3.7 vol.% of methanol diluted in pure helium (total flow rate of 20 mL/min) was supplied into the reactor by the isothermal saturator (0 °C). The reaction products were analyzed using a gas chromatograph (SRI 8610C) equipped with methanizer and FID detector.

3. Results and discussion

The X-ray diffraction patterns recorded in the low-angle range for pure SBA-15 and its modification with alumina species (SBA-15-SO₃H-Al) are shown in Fig. 1A. The characteristic reflections (corresponding to (100), (110) and (200) planes), typical of the 2D hexagonally structured pore system, were detected in the 2θ range of 0.9–2.1° for both the studied SBA-15 samples [35]. Thus, it proved that anchoring of MPTMS and its oxidation with H₂O₂ as well as deposition of alumina species did not damaged the hexagonal porous structure of the SBA-15 support. Fig. 1B presents XRD patterns recorded for MCF and its modifications. The pattern of MCF consists of one strong reflection at 2θ about 0.6 typical of this type of mesoporous silica with ultra-large pore dimensions. The occurrence of this reflection is an indication of the narrow size distribution of the spherical cells [36,37]. Moreover, it should be

noted that anchoring of MPTMS and its oxidation with H₂O₂ as well as deposition of alumina species did not damaged the hexagonal MCF porous structure.

The nitrogen adsorption-desorption isotherms recorded for pure silica supports and their modifications with alumina are presented in Fig. 2A (materials based on SBA-15) and 2B (materials based on MCF), respectively. The SBA-15 and MCF based samples exhibits the type IV adsorption-desorption isotherm, which is typical of mesoporous materials (IUPAC). The hysteresis loops recorded for the SBA-15 based samples are type the H1, characteristic of the presence of uniform, cylindrical and both side opened mesopores [38]. On the other hand, a series of MCF materials exhibits the hysteresis loops that can be classified as type H2. It indicates that the distribution of pore size and its shape is not well-defined. After deposition of alumina species, in case of all modified silica materials, total amount of adsorbed nitrogen decreased. This phenomenon is related to deposition of Al species inside the pores of SBA-15 or MCF.

The BET surface area, total pore volume and pore diameter of the studied samples are presented in Table 1. After modification of the silica supports with alumina their textural parameters significantly decreased. It should be noted that the average pore diameter decreased after deposition of alumina species into SBA-15 and MCF, what is possibly related to the location of these species inside of the silica materials pores.

The samples based on SBA-15 and MCF modified with MPTMS were analyzed by FT-IR spectroscopy. The obtained spectra are presented in Fig. 3. The silica supports exhibit characteristic bands at 3000–3800, 1000–1260 and 815 cm⁻¹ due to O–H of the silanol

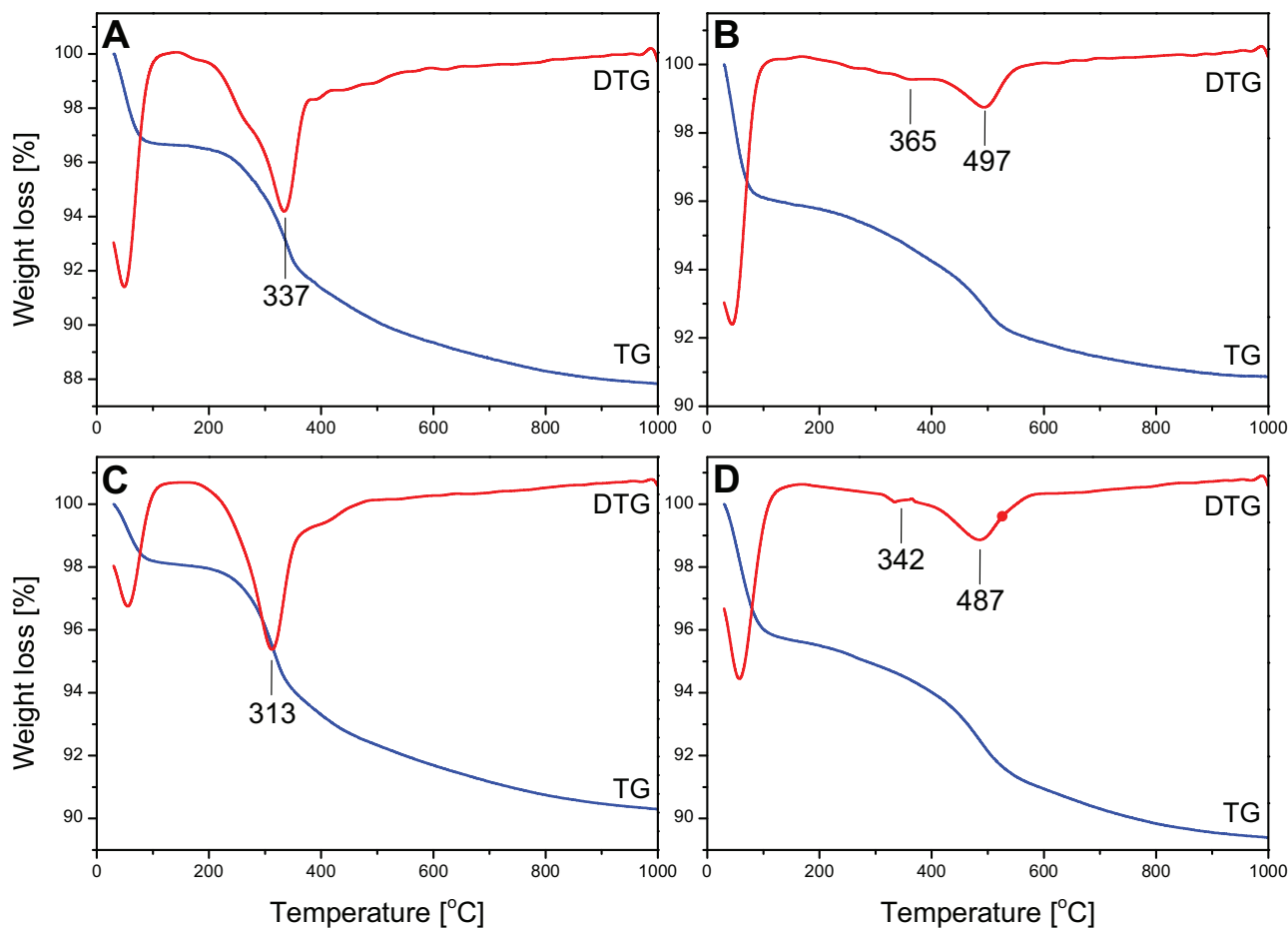


Fig. 4. TG-DTG profiles of (a) SBA-15-SH, (b) SBA-15-SO₃H, (c) MCF-SH, (d) MCF-SO₃H obtained in air atmosphere.

Table 2
Results of sulfur analysis in silica materials modified with surface functional groups.

Sample	Sulfur content (wt.%)	Functional group concentration (mmol/g)
SBA-15-SH	3.74	1.168
SBA-15-SO ₃ H	3.23	1.006
MCF-SH	1.68	0.524
MCF-SO ₃ H	1.22	0.381

groups, adsorbed water molecules and Si—O—Si stretching vibrations, respectively [39]. The spectra recorded for propylthiol-functionalized materials (SBA-15-SH and MCF-SH) possess additional bands centered at about 2940 and 2850 cm⁻¹ characteristic for C—H stretching vibrations in the propyl chains. Moreover, an additional weak band centered at 2580 cm⁻¹, typical of S—H stretching vibrations, is present in case of both the propylthiol-functionalized samples, what proves the successful anchoring of MPTMS on the silica surface [39]. This band is absent in FT-IR spectra of SBA-15-SO₃H and MCF-SO₃H, what confirms high efficiency of the applied oxidation step.

Fig. 4 shows the results of TG and DTG analyses of the SBA-15 and MCF supports modified with MPTMS before and after oxidation with H₂O₂. In each case a peak (centered below 100 °C) related to desorption of water was observed. The presence of mercaptopropyl species in the functionalized samples (Fig. 4A and C) is confirmed by very distinct peaks centered at 337 and 313 °C in DTG curves [39]. On the other hand, in DTG profiles recorded for SBA-15-SO₃H and MCF-SO₃H (Fig. 4B and D, respectively) the peaks in the range characteristic of thermal decomposition of alkylsulfonic groups (centered at 497 and 487 °C) were detected [40]. The loss of the remaining mercaptopropyl species in the samples oxidized with H₂O₂ may correspond to small peaks observed at 365 and 342 °C. Thus, the results of TG and DTG analyses clearly show that MPTMS was successfully anchored on the surface of mesoporous silicas and in the next step were oxidized to alkylsulfonic groups.

The results of elemental analysis (Table 2) of sulfur allowed to determine the content of —SH and —SO₃H groups in the samples modified with MPTMS before and after oxidation with H₂O₂. Assuming uniform distribution of the functional groups in the mesoporous silica supports, the surface concentration equals about 1.23 —SH and 1.06 —SO₃H μmol/m² in case of functionalized SBA-15 and 0.74 —SH and 0.54 —SO₃H μmol/m² in case of functionalized MCF. Thus, during oxidation process about 14% and

27% of the functional groups were removed from the SBA-15 and MCF surface, respectively.

Fig. 5 presents the ²⁷Al MAS NMR spectra recorded for the calcined samples doped with alumina species. The spectra of SBA-15-SO₃H-Al and MCF-SO₃H-Al contain signals characteristic for octahedral Al(VI) and tetrahedral Al(IV) around 5.8 and 62 ppm, respectively. Moreover, a signal at about 35.1 ppm appeared in the spectra of alumina modified silicas. According to various reports [41–44] this signal is attributed to pentacoordinated Al(V) or to an Al atom in highly distorted tetrahedral coordination. Very similar results, with respect to positions and relative intensities of signals, were reported by various authors for alumina species formed by thermal decomposition of aluminum Al13 Keggin oligocations [e.g. 41]. Thus, it could be concluded that alumina was deposited on the silica support mainly in the form of aluminum oligomeric species, which during calcination were transformed to Al₂O₃ aggregates.

STEM image and EDX maps of aluminum and silicon distribution recorded for SBA-15-SO₃H-Al before and after calcination are presented in Fig. 6A and B, respectively. It should be noted that the hexagonal porous structure of SBA-15 was not destroyed during deposition of aluminium species. Moreover, EDX images show the uniform distribution of aluminium in the sample, suggesting the presence of aluminium species also inside the pores of the SBA-15 support. Moreover, it can be seen that calcination of the SBA-15-SO₃H-Al sample did not result in significant sintering of alumina oligomeric species.

The surface acidity of the samples was studied by temperature-programmed desorption of ammonia (Fig. 7A and B). Only a very small amount of ammonia desorbed from both the SBA-15 and MCF silica supports at lower temperatures (below 200 °C). It can be seen that deposition of alumina species significantly increased the surface acidity of SBA-15 and MCF. In NH₃-TPD profiles recorded for the modified silica samples two peaks corresponding to ammonia bounded to weaker (centered at about 180 °C) and stronger acid sites (centered at about 300 °C) were found. For comparison also NH₃-TPD profile obtained for γ-Al₂O₃ is presented in Fig. 7A. It could be clearly seen that the amount of ammonia chemisorbed on this reference sample, and therefore concentration of surface acid sites (normalized to 1 g of the sample), is much lower in comparison to alumina modified silicas.

Surface concentration and surface density of acid sites as well as the Si to Al molar ratio and the molar ratio of Al to concentration of the surface acid sites is presented in Table 3. As it was shown by NH₃-TPD studies of the silica samples, their acidity was generated by deposition of aluminum species, while the concentration of acid sites on the surface of the pure silica supports was negligible. Thus, assuming that surface acidity is related only to the presence of aluminum species it was found that the molar ratio of deposited aluminum to the content of surface acidic groups is 7.2 for SBA-15-SO₃H-Al and 10.6 for MCF-SO₃H-Al. Such results show that alumina species were deposited in the form of aggregated species, what was intention of the presented studies.

Acidic catalysts are known to be active in the process of DME synthesis from methanol, therefore the studies of surface acidity were extended to determination of the chemical nature of acid sites. Distinguishing between Brønsted and Lewis acid sites was possible by FT-IR analysis of the samples pre-adsorbed with pyridine. The results are presented in Table 4. The total concentration of acid sites in SBA-15-SO₃H-Al and MCF-SO₃H-Al was determined by adsorption and evacuation of pyridine at 130 °C. First of all, it should be noted that the obtained values are only slightly smaller than that determined by NH₃-TPD method (presented in Table 3). These differences can be related to lower temperature (70 °C) of ammonia sorption applied in NH₃-TPD method. Another explanation could be different kinetic diameter of ammonia and pyridine molecules and therefore different

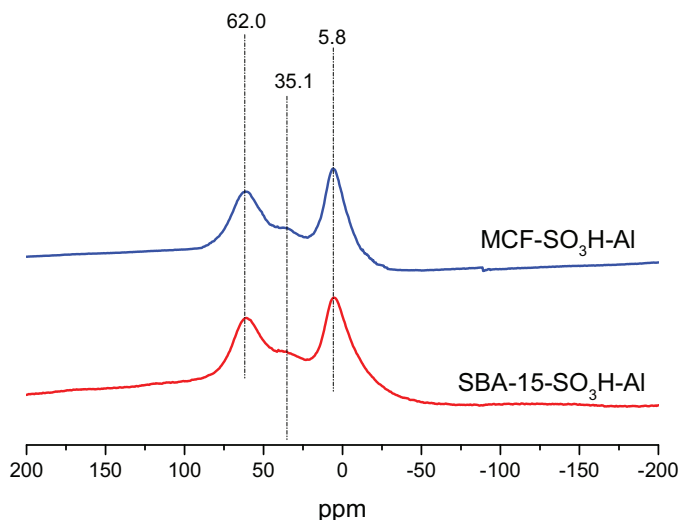
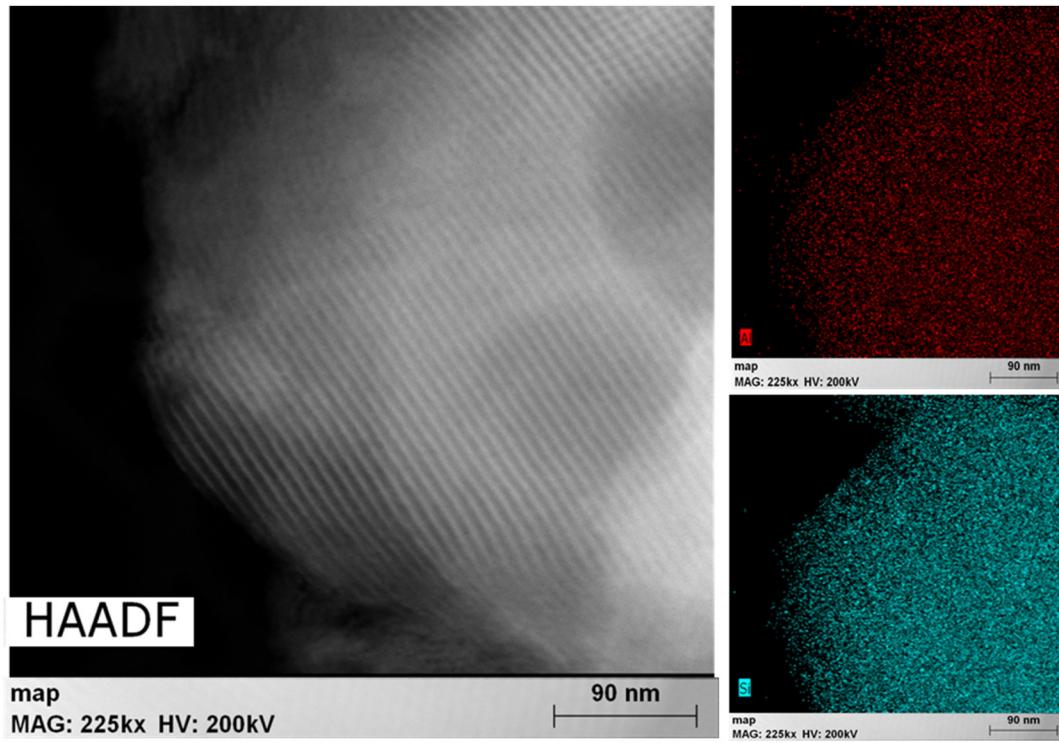


Fig. 5. ²⁷Al MAS-NMR spectra for SBA-15-Al, SBA-15-SO₃H-Al.

A)



B)

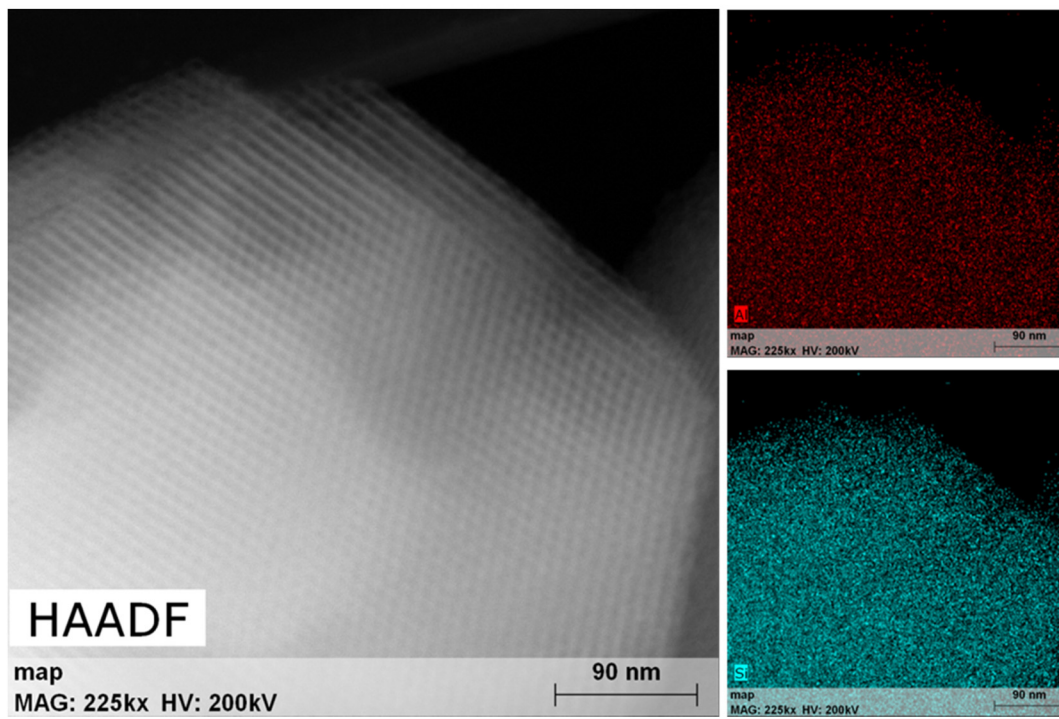


Fig. 6. STEM image and EDX elements distribution maps recorded for SBA-15-SO₃H-Al before (a) and after (b) calcination.

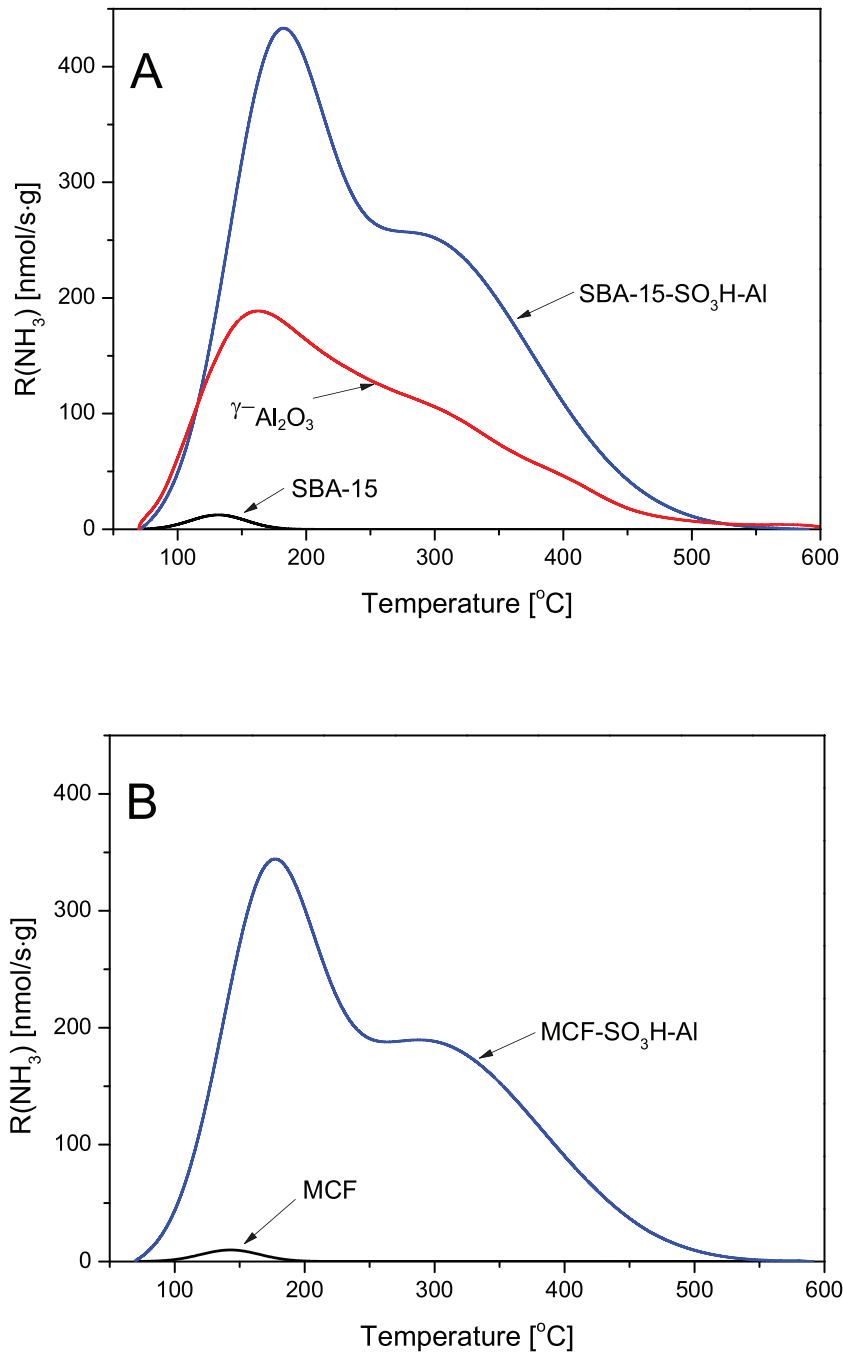


Fig. 7. NH₃-TPD profiles of the pure silica supports and their modifications with alumina species. Conditions: weight of sample—50 mg; sorption—1.0 vol.% NH₃ in He, gas flow—20 mL/min; desorption flow of He—20 mL/min.

Table 3

Surface concentration (C_A), surface density (D_A) of acid sites and the Si/Al ratio in the modified silica materials.

Sample	C_A ($\mu\text{mol/g}$)	D_A ($\mu\text{mol/m}^2$)	Si/Al ratio	Al/ C_A (mol/mol)
SBA-15	5	0.01	-	-
SBA-15-SO ₃ H-Al	519	0.89	4.08	7.2
MCF	4	0.01	-	-
MCF-SO ₃ H-Al	412	0.81	3.42	10.6
γ -Al ₂ O ₃	177	0.69	0.00	110.8

Table 4

Total surface concentration (C_A) of acid sites, concentration of Brønsted (C_B) and Lewis (C_L) types of acid sites determined by FTIR of pyridine pre-adsorbed samples evacuated at 130 and 330°C.

Sample	130°C		330°C	
	C_A ($\mu\text{mol/g}$)	C_B : ($\mu\text{mol/g}$) C_L : ($\mu\text{mol/g}$)	C_A ($\mu\text{mol/g}$)	C_B : ($\mu\text{mol/g}$) C_L : ($\mu\text{mol/g}$)
SBA-15-SO ₃ H-Al	450	C_B : 104 C_L : 346	272	C_B : 30 C_L : 242
MCF-SO ₃ H-Al	407	C_B : 77 C_L : 330	222	C_B : 32 C_L : 190

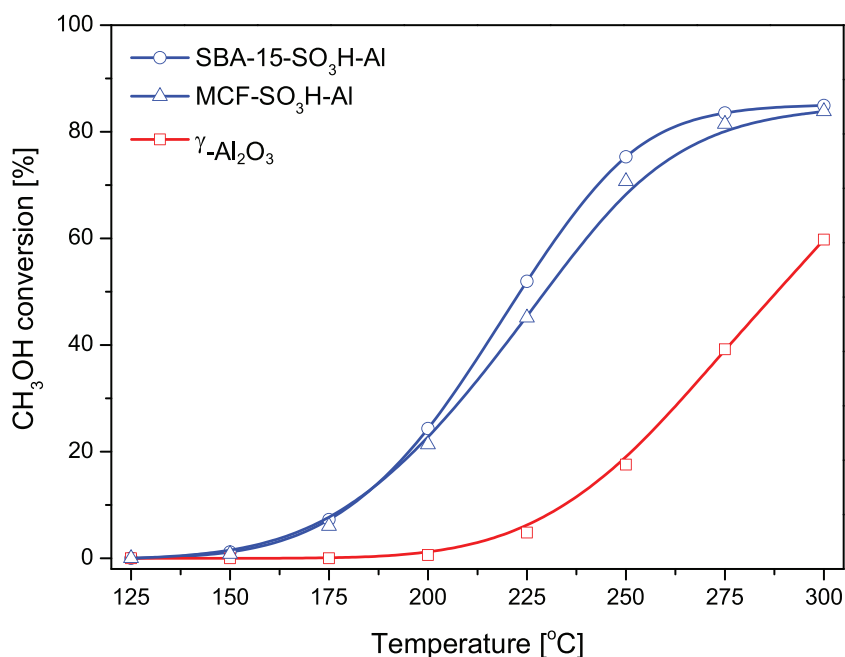


Fig. 8. Temperature dependence of CH₃OH conversion to DME over the pure silica supports and their modifications with alumina species. Conditions: weight of sample—100 mg, 4.0 vol.% CH₃OH, He as balancing gas, total flow rate—20 mL/min.

accessibility of these molecules into acid sites located in pores, especially micropores. Lowered accessibility of acid sites for pyridine molecules in comparison to ammonia ones in mesoporous aluminosilicates of various origin has been widely discussed [45]. An important issue could be differences in acid strength of both these molecules. It should be also noted that the content of acid sites in the SBA-15-SO₃H-Al samples is higher than in MCF-SO₃H-Al, what is consistent with results of NH₃-TPD studies. In both the samples Lewis acid sites significantly dominated over Brønsted sites. An increase in evacuation temperature to 330 °C reduced the surface concentration of chemisorbed pyridine by ca. 40–45%. Also in this case Lewis acid sites dominated over Brønsted sites, however differences in the contribution of both types of acid sites become more significant than at 130 °C. Thus, it could be concluded that Lewis acid sites are characterized by higher acidic strength than Brønsted sites.

The results of the catalytic studies of the MTD process over the pure silica supports and their modifications with alumina species are shown in Fig. 6. It should be noted that under reaction conditions, in the presence of the modified silica samples, methanol was converted to DME with a very high selectivity (nearly 100%). Thus, only the conversion of methanol is presented and discussed. The pure silica supports (SBA-15 and MCF) were catalytically inactive in the studied temperature range. Deposition of alumina species activated silica mesoporous materials for the catalytic conversion of methanol to DME. In this case reaction started at temperature as low as 125 °C and continuously increased reaching above 80% of methanol conversion at 300 °C. There is some differences in catalytic activity of the alumina modified silica supports. The catalysts based on SBA-15 is more active than that obtained from MCF. Another important issue is a nature and optimal strength of acid sites active in the process of methanol conversion into DME. As it was shown by Py-FTIR studies, both Brønsted and Lewis acid sites are present in the silica based catalysts and can operate in the studied temperature range. Moreover, the results of Py-FTIR confirmed that the total amount and strength of Lewis acid sites in the obtained catalysts is much higher in comparison to the total amount of Brønsted acid sites. Assuming similarity of the active sites in the synthesized materials

to active sites in γ-Al₂O₃, commercially used in the MTD process, the catalytic activity of the catalysts is associated with the presence of the Lewis acid sites [20,46]. Thus, it seems that the DME synthesis from methanol over the Brønsted acid sites in case of the studied materials is less important. In Fig. 8, apart from the mesoporous silica based catalysts, also results of the catalytic test performed for commercial γ-Al₂O₃ are shown. It can be clearly seen that both mesoporous silicas modified with alumina species are significantly more active comparing to γ-Al₂O₃. This comparison shows that the studied catalytic materials are promising for potential application in conversion of methanol to DME. Such significant differences in catalytic activity of γ-Al₂O₃ and both the silica based catalysts is possibly related to the surface concentration of acid sites, which is much higher in case of SBA-15-SO₃H-Al and MCF-SO₃H-Al, due to dispersion of large number of alumina aggregates on a very large silica surface of the studied samples. Another important property of the SBA-15 and MCF supports is their mesoporous structure, that consists of relatively large pores that guarantees fast internal diffusion of the reactants.

4. Conclusions

The catalysts based on the high surface area silica supports (SBA-15, MCF) modified with aggregated alumina species were tested in the methanol dehydration to DME. The alumina oligocations were deposited on the silica surface functionalization with organic groups by ion-exchange method. The alumina modified materials were found to be active and selective catalysts in the MTD process. Among the studied samples the best catalytic results were obtained for mesoporous SBA-15 silica doped with alumina. High catalytic activity of these samples was related to high content of the surface acid sites, mainly Lewis type, and their optimal strength as well as the mesoporous structure of the catalysts that guarantees fast internal diffusion of the reactants.

Acknowledgements

The studies were carried out in the frame of project 2012/05/B/ST5/00269 from the National Science Centre (Poland). Part of the

research was done with equipment purchased in the frame of European Regional Development Fund (Polish Innovation Economy Operational Program—contract no. POIG.02.01.00–12–023/08).

References

- [1] S.P. Naik, V. Bui, T. Ryu, J.D. Miller, W. Zmierczak, *Appl. Catal. A: Gen.* 381 (2010) 183–190.
- [2] C.T. Kresge, M.E. Leonowicz, W.J. Roth, J.C. Vartuli, J.S. Beck, *Nature* 359 (1992) 710–712.
- [3] A. Taguchi, F. Schüth, *Micropor. Mesopor. Mater.* 77 (2005) 1–45.
- [4] L. Chmielarz, P. Kuśtrowski, R. Dziembaj, P. Cool, E.F. Vansant, *Appl. Catal. B: Environ.* 62 (2006) 369–380.
- [5] T. Linsen, K. Cassiers, P. Cool, E.F. Vansant, *Adv. Colloid Interface Sci.* 103 (2003) 121–147.
- [6] L. Chmielarz, P. Kuśtrowski, R. Dziembaj, P. Cool, E.F. Vansant, *Micropor. Mesopor. Mater.* 127 (2010) 133–141.
- [7] L. Chmielarz, P. Kuśtrowski, M. Drozdek, M. Rutkowska, R. Dziembaj, M. Michalik, P. Cool, E.F. Vansant, *J. Porous Mater.* 18 (2011) 483–491.
- [8] P. Kuśtrowski, Y. Segura, L. Chmielarz, J. Surman, R. Dziembaj, P. Cool, E.F. Vansant, *Catal. Today* 114 (2006) 307–313.
- [9] M. Xu, J.H. Lunsford, D.W. Goodman, A. Bhattacharyya, *Appl. Catal. A: Gen.* 149 (1997) 289–301.
- [10] T. Takeguchi, K. Yanagisawa, T. Inui, M. Inoue, *Appl. Catal. A: Gen.* 192 (2000) 201–209.
- [11] A.A. Rownaghi, F. Rezaei, M. Stante, J. Hedlund, *Appl. Catal. B: Environ.* 119–120 (2012) 56–61.
- [12] F. Yaripour, F. Baghaei, I. Schmidt, J. Perregaard, *Catal. Commun.* 6 (2005) 147–152.
- [13] F.S. Ramos, L.E.P. Duarte de Farias, J.L. Borges, M.A. Monteiro, E.F. Sousa-Aguiar, L.G. Appel, *Catal Today* 101 (2005) 39–44.
- [14] M. Stiefel, R. Ahmad, U. Arnold, M. Döring, *Fuel Process. Technol.* 92 (2011) 1466–1474.
- [15] J. Fei, Z. Hou, B. Zhu, H. Lou, X. Zheng, *Appl. Catal. A: Gen.* 304 (2006) 49–54.
- [16] D. Jin, B. Zhu, Z. Hou, J. Fei, H. Lou, X. Zheng, *Fuel* 86 (2007) 2707–2713.
- [17] K.C. Tokay, T. Dogu, G. Dogu, *Chem. Eng. J.* 184 (2012) 278–285.
- [18] J. Abu-Dahrieh, D. Rooney, A. Goguet, Y. Saih, *Chem. Eng. J.* 203 (2012) 201–211.
- [19] S. Alamolhoda, M. Kazemeini, A. Zaherian, M.R. Zakerinasab, *J. Ind. Eng. Chem.* 18 (2012) 2059–2068.
- [20] D.M. Sung, Y.H. Kim, E.D. Park, J.E. Yie, *Catal. Commun.* 20 (2012) 63–67.
- [21] H. Knözinger, K. Kochloeff, W. Meye, *J. Catal.* 28 (1973) 69–75.
- [22] J.E. Dabrowski, J.B. Butt, H. Bliss, *J. Catal.* 18 (1970) 297–313.
- [23] J. Bandiera, C. Naccache, *Appl. Catal.* 69 (1991) 139–148.
- [24] Z. Hosseini, M. Taghizadeh, F. Yaripour, *J. Nat. Gas Chem.* 20 (2011) 128–134.
- [25] B. Sabour, M.H. Peyrovi, T. Hamoule, M. Rashidzadeh, *J. Ind. Eng. Chem.* 20 (2014) 222–227.
- [26] S. Bhattacharya, K.B. Kabir, K. Hein, *Prog. Energy Combust.* 39 (2013) 577–605.
- [27] S.J. Royae, C. Falamaki, M. Sohrabi, S.S.A. Talesh, *Appl. Catal. A: Gen.* 338 (2008) 114–120.
- [28] Y. Tavara, S.H. Hosseini, M. Ghavipour, M.R.K. Nikou, A. Shariati, *Chem. Eng. Process.* 73 (2013) 144–150.
- [29] N. Khandan, M. Kazemeini, M. Aghaziarati, *Appl. Catal. A: Gen.* 349 (2008) 6–12.
- [30] S. Damyanova, B. Pawelec, K. Arishtirova, J.L. Fierro, C. Sener, T. Dogu, *Appl. Catal. B: Environ.* 92 (2009) 250–261.
- [31] V. Meynen, P. Cool, E.F. Vansant, *Micropor. Mesopor. Mater.* 125 (2009) 170–223.
- [32] M. Trejda, K. Stawicka, A. Dubińska, M. Ziolek, *Catal. Today* 187 (2012) 129–134.
- [33] L. Chmielarz, P. Kuśtrowski, M. Michalik, B. Dudek, Z. Piwowska, R. Dziembaj, *Catal. Today* 137 (2008) 242–246.
- [34] K. Sadowska, K. Góra-Marek, J. Datka, *Vibr. Spec.* 63 (2012) 418–425.
- [35] R. Ghorbani-Vaghei, S. Hemmati, H. Veisi, *J. Mol. Catal. A: Chem.* 393 (2014) 240–247.
- [36] Y. Su, Y.-M. Liu, L.-C. Wang, M. Chen, Y. Cao, W.-L. Dai, H.-Y. He, K.-N. Fan, *Appl. Catal. A: Gen.* 315 (2006) 91–100.
- [37] O. Aktas, S. Yasierlia, G. Dogua, T. Dogu, *Mater. Chem. Phys.* 31 (2011) 151–159.
- [38] S. Lowell, J.E. Shields, M.A. Thomas, M. Thommes, *Particle Technol. Ser.* 16 (2004) .
- [39] L. Saikia, D. Srinivas, P. Ratnasamy, *Micropor. Mesopor. Mater.* 104 (2007) 225–235.
- [40] D. Margolese, J.A. Melero, S.C. Christiansen, B.F. Chmelka, G.D. Stucky, *Chem. Mater.* 12 (2000) 2448–2459.
- [41] L. Storaro, M. Lenarda, M. Perissinotto, V. Lucchini, R. Ganzerla, *Micropor. Mesopor. Mater.* 20 (1998) 317–331.
- [42] A.M. de Andres, J. Merino, J.C. Galvan, E. Ruiz-Hitzky, *Mater. Res. Bull.* 34 (1999) 641–651.
- [43] C. Belver, P. Aranda, M.A. Martín-Luengo, E. Ruiz-Hitzky, *Micropor. Mesopor. Mater.* 147 (2012) 157–166.
- [44] J.H. Kwak, J.Z. Hu, D.H. Kim, J. Szanyi, C.H.F. Peden, *J. Catal.* 251 (2007) 189–194.
- [45] K. Góra-Marek, M. Derewiński, P. Sarv, J. Datka, *Catal. Today* 101 (2005) 131–138.
- [46] Z.-J. Zuo, W. Huang, P.-D. Han, Z.-H. Gao, Z. Li, *Appl. Catal. A: Gen.* 408 (2011) 130–136.
ce:surname>Han, Z.-H.Gao, Z.Li, *Appl. Catal. A: Gen.*, 408(2011) 130136.